

See discussions, stats, and author profiles for this publication at: <https://www.researchgate.net/publication/239658650>

# The Kinetic Friction of Ice

Article in *Proceedings of The Royal Society A* · January 1976

DOI: 10.1098/rspa.1976.0013

---

CITATIONS

139

READS

281

3 authors, including:



**John Frederick Nye**  
University of Bristol

253 PUBLICATIONS 15,967 CITATIONS

SEE PROFILE

Some of the authors of this publication are also working on these related projects:



electromagnetic probe [View project](#)



glaciology [View project](#)

*Proc. R. Soc. Lond. A.* **347**, 493–512 (1976)*Printed in Great Britain*

## The kinetic friction of ice

BY D. C. B. EVANS,† J. F. NYE AND K. J. CHEESEMAN‡

*H. H. Wills Physics Laboratory, Bristol, England**(Communicated by F. C. Frank, F.R.S. – Received 6 January 1975 –**Revised 16 July 1975)*

[Plate 5]

An apparatus based on a pendulum hanging around a revolving drum of ice was developed to measure the kinetic friction between a slider and an ice surface under conditions commonly experienced in ice skating (temperatures from  $-15$  to  $-1$  °C and velocities from  $0.2$  to  $10$  m s $^{-1}$ ). The results are explained by a quantitative development of the frictional heating theory of Bowden & Hughes (1939): heat produced by friction raises the surface to its melting point and a small amount of water is produced which lubricates the contact area. The frictional heat used in melting is usually small; most of the heat flows from the contact area at the melting point into the slider and into the ice. This makes it possible to calculate the dependence of the coefficient of friction  $\mu$  on the thermal conductivity of the slider, the ambient temperature and the velocity of sliding  $v$ , without considering the detailed mechanism that produces the frictional force. For sliders of mild steel and Perspex the main heat loss is through the ice and  $\mu$  is hence proportional to the temperature below the melting point and to  $v^{-\frac{1}{2}}$ . For these two materials the magnitude of the coefficient of friction is correctly calculated from measured and known parameters to within a factor of 2. The remaining discrepancy is probably mainly due to the difference between the real and apparent contact areas. For a copper slider the heat loss through the metal is about the same as that through the ice. There is no pressure melting in these experiments; the only effect of the lowering of the melting point by pressure is to reduce slightly the frictional heat needed to keep the contact area at the melting point. On the other hand, at temperatures above about  $-2$  °C pressure melting would be expected.

### 1. INTRODUCTION

The coefficient of kinetic friction of ice, measured under conditions of ice skating, is 10–100 times smaller than for most common materials. Among several theories of the effect two may be specially mentioned. Reynolds (1901) pointed out that water expands on freezing, and suggested that pressure-melting produces a lubricating film of water. It was difficult to calculate the pressure between the slider and the ice surface because the true area of contact was uncertain, but it seemed possible that the melting point was lowered locally by several degrees. The theory

† Present address: New Cavendish Laboratory, Cambridge, England.

‡ Present address: Schlumberger, 42 Rue Saint-Dominique, Paris, 7e, France.

readily agreed with the fact that sliding becomes more difficult as the temperature is decreased. Bowden & Hughes (1939), on the other hand, concluded from experiments that the low friction was due to a thin lubricating water film produced largely by frictional heating. They showed that the electrical conductivity measured between two electrodes set in one of the surfaces during sliding was consistent with the presence of a water film about  $70\ \mu\text{m}$  thick. If the lubricating film were formed by frictional heating, lowering the ambient temperature or increasing the thermal conductivity of the skate would make the water film more difficult to form and would thus increase the coefficient of friction – which is the behaviour they observed.

Much other work on the kinetic friction of both ice and snow has recently been critically reviewed by Mellor (1974). The Bowden & Hughes theory continues to be widely accepted, but it has not been developed analytically to a point where it can fully explain the effects of temperature, velocity, load and slider material on the coefficient of friction. We describe here a series of experiments, made with a new design of apparatus, to find how the coefficient of friction depends on these parameters. We then give an analytical development of the frictional melting theory based on a consideration of the heat flows. The main heat losses are shown to be through the slider and through the ice, and by assuming that the contact area is at the melting point one can calculate these heat flows, and hence the friction. This theory accounts for the way the friction depends on the conductivity of the slider, on the temperature and on the velocity, and it predicts the magnitude of the coefficient of friction correctly within a factor of 2. We suggest that the remaining discrepancy is probably mostly due to the difference between the real and apparent contact areas.

## 2. APPARATUS

To measure the frictional properties of ice in a range appropriate to skating, we used velocities up to  $10\ \text{m s}^{-1}$  (22 mile/h) and temperatures between  $-1$  and  $-15\ ^\circ\text{C}$ . The apparatus (figure 1) was designed to measure coefficients of friction down to 0.01 with an accuracy of a few percent. It consisted of a drum of ice,  $F$ , mounted with its axis horizontal and revolving at constant speed, with two sliders  $D$ , supported on its surface by a pendulum frame  $E$  made of Perspex. The frictional forces on the sliders make the pendulum rotate through a small angle  $\theta$  from its equilibrium position, their magnitude being proportional to  $\sin \theta$ , which was measured with an optical lever about 2 m long. The advantage of a pendulum is that it removes the need for any additional mechanical constraints, which would produce unwanted forces. The sensitivity (deflexion per unit force) could be adjusted by altering the position of the weights  $G$ , and the whole apparatus was enclosed in a top-opening refrigerator.

The most successful way of making the ice drum was first to freeze ordinary tap water in a large polythene film cylinder by lowering it into a refrigerator at  $1\ \mu\text{m s}^{-1}$ . A short length was sawn off the cylinder, frozen to a chuck and turned to a true cylinder surface with a chisel. The outer surface was then free from cracks and

bubbles—an essential condition for smooth running. Such cylinders could be used for several hours without deteriorating.

A real ice skate has sharp edges, sometimes a hollow-ground cross-section and usually a small longitudinal curvature (figure 2*a*); the contact between a skate and a flat ice surface is thus complicated and ill-defined. To simplify the geometry of the contact and eliminate the effects of sharp edges, we used straight rods of circular cross-section, 10 mm in diameter, held in contact with the cylindrical ice surface

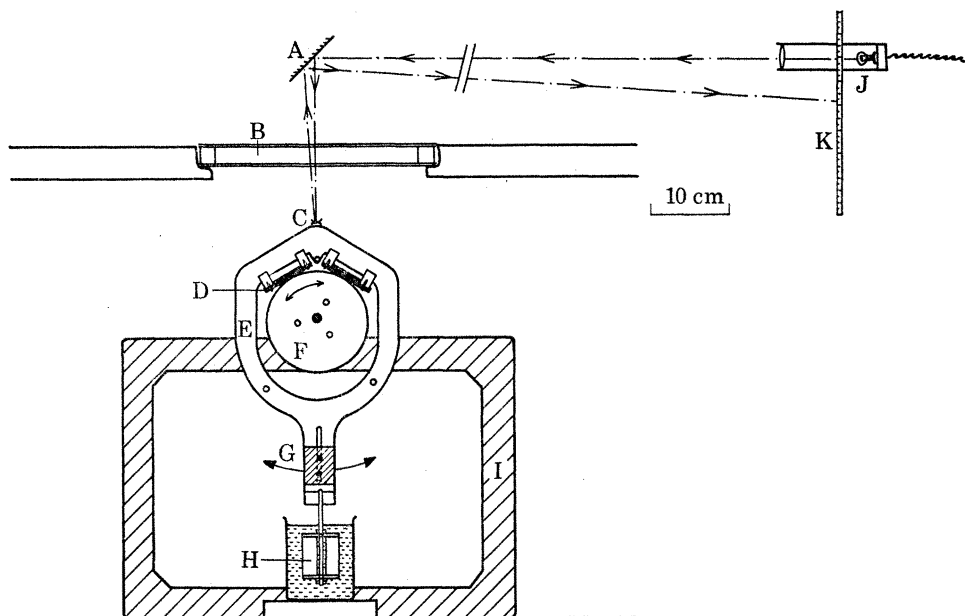


FIGURE 1. The apparatus for measuring kinetic friction. A, Plane mirror; B, Perspex window; C, concave mirror; D, rod; E, pendulum; F, ice drum; G, brass weights; H, damping vane; I, supporting frame; J, lamp; K, scale.

(the axes of the sliders being perpendicular to the axis of the ice cylinder). These were the main experiments and we hoped that the well-defined conditions might enable us to develop a quantitative theory. But in order to study how applicable the results using rods might be to the problem of ice skating, we also did an experiment which modelled more closely a real skate in action. A curved ice skate (figure 2*b*) of mild steel with a width of 5 mm was hollow ground to a radius of 25 mm. The skate-like edge had a longitudinal curvature of radius 60 mm to fit fairly closely to the cylindrical surface of the ice drum. A shallow trench was then accurately machined in the ice drum to a radius of 54 mm so that the difference in curvature between this 'skate' and the ice matched the difference in curvature between a real skate and a flat ice surface (figures 2*a*, *b*).

To make the pendulum laterally stable while using the rods, we had to run them in a 90° V-shaped groove cut into the cylinder; thus each rod had two points of contact with the ice, one on either side of the groove. Clearly both rods run in the same

tracks and there might have been difficulties if, after passing under one rod, the tracks did not have time to return to the normal temperature of the ice block before passing under the other. Calculations showed that at the velocities used there was no danger of this happening; the presence of one rod could not significantly affect the ice temperature under the other.

When the pendulum was tested on the ice two sorts of unwanted oscillations appeared. The first was simply due to slight irregularities in the track; high frequency vibrations were produced, especially at high speeds, which made the ice surface deteriorate rapidly; to prevent them the rods were cushioned with 2 mm rubber sheeting. The second type of oscillation was caused by the fact that friction



FIGURE 2. The contact between a curved skate and the ice surface in (a) real ice skating, (b) this experiment.

decreases with increasing velocity; it is easy to show that this produces unstable oscillations of the pendulum about the axis of the drum, the effect being that of a negative damping coefficient. These oscillations predominated at low velocities where the rate of change of friction with velocity is greatest; they were successfully damped by a vane,  $H$ , attached to the pendulum and immersed in a brine dash pot.

### 3. EXPERIMENTS AND RESULTS

#### 3.1. Measurement of frictional force

The torque of the frictional forces on the pendulum is equal to the restoring torque of the pendulum's weight. This gives a relation between the coefficient of friction  $\mu$  and the angular deflexion  $\theta$

$$4\mu Lr = Wl \sin \theta, \quad (1)$$

where  $L$  is the normal reaction of each of the four areas of contact,  $r$  is the radius of the V-groove,  $W$  is the weight of the pendulum, and  $l$  is the distance between the axis of the drum and the centre of gravity of the pendulum.

When the angular deflexion of the pendulum is small, the relation between  $L$  and  $W$  is

$$L = \frac{1}{4} W \operatorname{cosec} \frac{1}{2}\phi \operatorname{cosec} \frac{1}{2}\xi, \quad (2)$$

where  $\phi$  is the interior angle between the rods and  $\xi$  the angle of the V-groove. Combining (1) and (2) gives

$$\mu = (l/r) \sin \theta \sin \frac{1}{2}\phi \sin \frac{1}{2}\xi. \quad (3)$$

Static friction made it impossible to measure the position of the pendulum with no frictional torque present, so  $\theta$  was measured by reversing the direction of rotation of the drum and halving the angle between the two equilibrium positions. One limitation

of the apparatus as a representation of ice skating was that the sliders ran repeatedly over the same track, so observations of the friction between a slider and a virgin ice surface could not be made. However, measurements were made after as few as five revolutions of the drum and these gave slightly lower values of coefficient of friction than those obtained after a few minutes running. A complete run usually took about 30 min and reproducibility was good after the first minute.

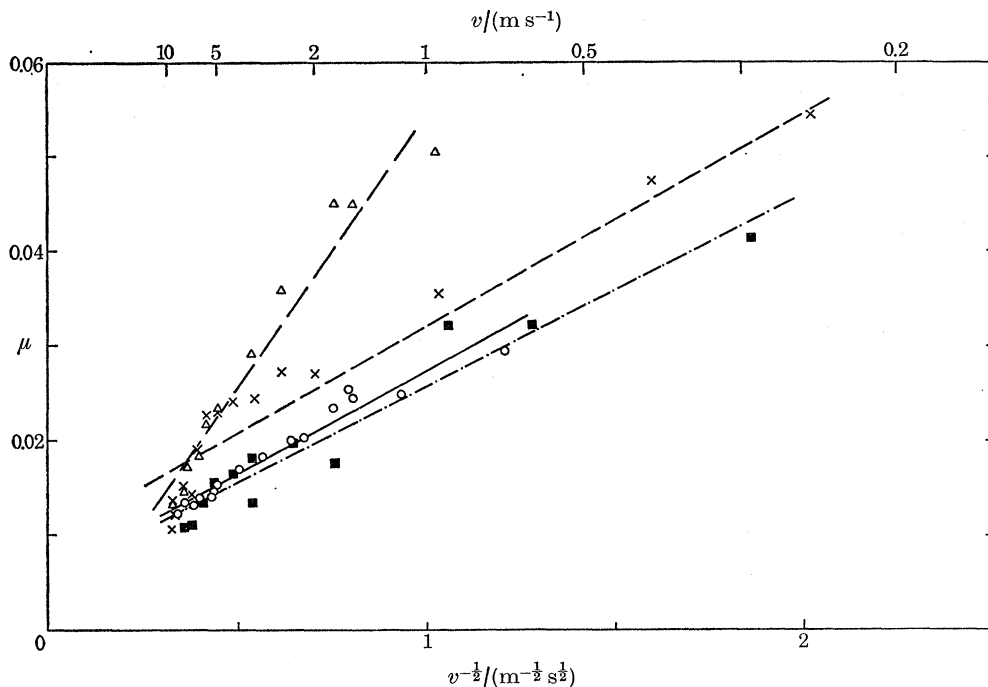


FIGURE 3. The variation of coefficient of friction with velocity for various rod materials and the curved skate. Air temperature  $-11.5^{\circ}\text{C}$ ; total normal load ( $4L$ ) is  $45.4\text{ N}$ .  $\Delta$ , (— —) copper rods;  $\blacksquare$  (- - - -) Perspex rods;  $\circ$  (—) mild steel rods;  $\times$  (- - - -) mild steel skate.

### 3.2. Variation of friction with velocity

Coefficient of friction  $\mu$  was measured at velocities  $v$  between  $0.2$  and  $10\text{ m s}^{-1}$  at an air temperature of  $-11.5^{\circ}\text{C}$  using  $10\text{ mm}$  diameter rods of mild steel, Perspex and copper. In these runs, successive readings were taken at random throughout the velocity range. Finally a run was made with the curved ice skate to compare its behaviour with that of the rods.

The results (figure 3) show that  $\mu$  increases approximately linearly with  $v^{-1/2}$  in all four cases. The mild steel skate caused considerable lack of stability of the pendulum; the readings for it show a rather greater scatter and a greater departure from the  $v^{-1/2}$  dependence, especially at the higher speeds. The friction of the mild steel skate is seen to be greater than that of the mild steel rod at the lower speeds but about the same at the higher speeds. A striking feature of the results is that at the highest speed used ( $10\text{ m s}^{-1}$ ) the three rods and the skate all have the same friction.

### 3.3 Variation of friction with temperature

The coefficient of friction was measured (figure 4) using mild steel, Perspex and copper rods at air temperatures between  $-1$  and  $-15$  °C; the velocity was constant at  $3.16 \text{ m s}^{-1}$ . Measurements were made while the temperature of the refrigerator was slowly rising and again as the temperature was steadily falling. The rates of heating and cooling were almost equal and a complete run took about 4 h. The maximum temperature was  $-1$  °C; rapid wear of the track occurred at higher temperatures. The temperature was recorded with a mercury thermometer held near the ice surface and there was hysteresis of from 2 to 5 °C between the heating and cooling sections of the runs. This has been allowed for by assuming that thermal equilibrium would give readings midway between the heating and cooling lines. The readings show a linear dependence of coefficient of friction on air temperature.

The copper rods gave a much larger scatter of readings than the steel or Perspex rods. This probably arose because a steady thermal state was not reached; it was noted that the temperature of the copper rods, measured with thermocouples embedded in them, depended to some extent on the past history of the run.

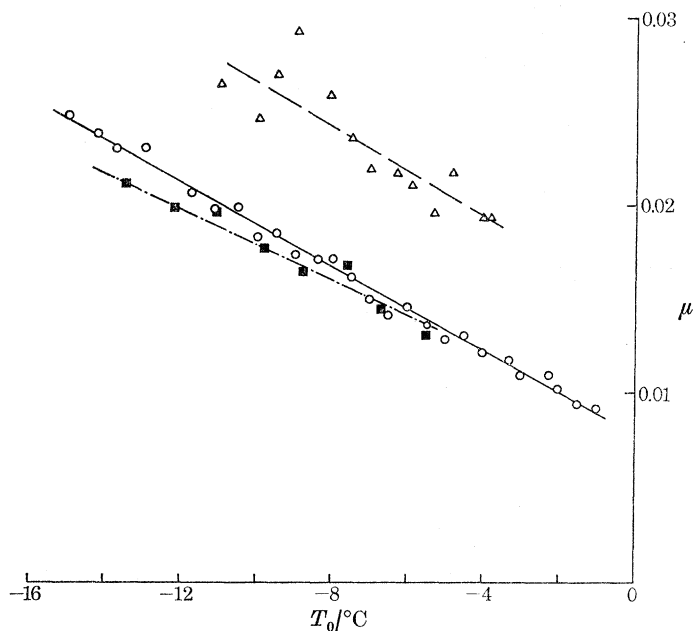


FIGURE 4. The variation of coefficient of friction with air temperature for various rod materials. Velocity  $3.16 \text{ m s}^{-1}$ , total normal load ( $4L$ ) is  $45.4 \text{ N}$ .  $\Delta$  (---) copper rods;  $\blacksquare$  (-·-·-) Perspex rods;  $\circ$  (—) mild steel rods.

### 3.4. Variation of friction with load

The frictional force was measured for values of  $L$ , the normal load on each of the four areas of contact, between 5 and 20 N, using mild steel rods and four well-spaced velocities. The loads were varied without changing the horizontal position of the



centre of gravity of the pendulum by adding weights to a scale pan suspended from the centre of gravity. The frictional force increased with larger loads but the coefficient of friction fell by about 40% over the range at each of the four velocities. This corresponds roughly to  $\mu \propto L^{-\frac{1}{2}}$ ; further work would be needed to establish the friction-load relation more precisely.

### 3.5. *Heat flow through the copper rods*

To obtain an idea of the effect of the conductivity of the rod material on the friction, an experiment was done to measure what fraction of the total heat produced at the contact area was dissipated through the rods. The temperature difference between the copper rods and the air, produced in a variation of temperature run, was measured with thermocouples embedded in the rods. The rate of heat loss to the air from the rod surfaces corresponding to this temperature difference, treated as uniform throughout the rod, was then found by a simple rate-of-cooling experiment. The total rate of production of heat at the areas of contact is the product of the total frictional force and the velocity of the ice. Comparison of the heat lost through the rods to the total heat produced showed that at  $3.16 \text{ ms}^{-1}$  between 40 and 60% of the heat was conducted away through the copper rods, the fraction being apparently independent of air temperature between  $-2^\circ\text{C}$  and  $-15^\circ\text{C}$ . The importance of conduction of heat through the rods will depend on the ice velocity and the rod material and is discussed further in §4.3.

### 3.6. *The size and nature of the contact areas*

At temperatures above  $-2^\circ\text{C}$ , the two ice tracks wore continuously. At lower temperatures wear was rapid at first, as the pressure exceeded the hardness of the ice, but after a few hundred traversals of the surface it quickly decreased. As long as the temperature was kept below  $-2^\circ\text{C}$  there was very little further wear even after as many as  $10^5$  revolutions; the width of each track was then between 1 and 2 mm.

To estimate the shape and size of the area of contact between the rods and the ice surface, we formed a track with a polished brass rod for a few minutes with  $L = 11 \text{ N}$ . This rod was then coated with a thin layer of soot from a candle and brought into contact with the ice surface again for a few seconds. The contact region (figure 5) shows an area where the carbon has been removed by the ice; it is roughly elliptical in shape, about 1.5 mm long and 0.6 mm wide, the motion of the ice being along the major axis of the ellipse from left to right. An interesting feature is the dark patch of carbon extending around the trailing edge. In colour the contrast is more striking and appears as a black patch on a brownish background. It was found that an identical change in the colour of the carbon coating could be achieved by wetting the surface with a little water and allowing it to dry. This is a strong indication that water is formed at the contact region. (The vertical lines in the contact area were present before the experiment.)

After a run the rods showed definite signs of abrasion at the areas of contact.



Abrasion was visible on rods of all the different materials but the effect on the Perspex rods was particularly interesting (figure 6). The whole contact region was covered in small cracks and scratches. Viewed with a stereo microscope the cracks were seen to extend up to 100  $\mu\text{m}$  into the surface and considerable pieces of Perspex were completely removed.

#### 4. THEORY AND DISCUSSION

In this section we suggest that the conduction of heat into the ice and, in the case of copper, into the slider is the process which largely determines the coefficient of friction under the conditions used in these experiments. By considering the conduction process we derive a relation between coefficient of friction, temperature and velocity in terms of readily measurable parameters which is found to agree with the experimental data. The relevance of the analysis to the problem of real ice skating is then briefly discussed.

##### 4.1. *The initial wear of the tracks*

Since the rods run in a V-shaped groove in the ice cylinder, the geometry of each of the four rod-ice contacts is that between a cylinder and a cone. Any such contact between a hard and relatively soft material produces an indentation under load in the softer material, in this case the ice; because the behaviour of ice under deformation is largely plastic, the indentation remains when the load is removed. The area of the indentation is equal to the load divided by the hardness of the ice. A track formed by rotation of the ice drum is essentially a series of indentations and the action is one of drawing a spoon across the surface of butter. One reason why the track is not completely formed in the first revolution of the drum is that even with a simple elastic-plastic solid the geometry met in the second transverse would be different from that met in the first (see Bowden & Tabor 1964, pp. 284–5, but note that their geometry is slightly different from ours). Another reason is that the hardness of the ice depends on the time of loading (Barnes & Tabor 1966). The formation of the track is therefore a gradual process but it is largely completed after a few hundred revolutions. Measurements of the area of contact (§3.6) showed that a load of 11 N was supported by an area of about 0.7 mm<sup>2</sup>; this gives a hardness of 15 MN m<sup>-2</sup>, which is within the range of values measured by Barnes & Tabor (1966). One might expect that the resistance due to ploughing of the rod through the ice would increase the friction while the track is being formed; we shall show that the friction is greatly influenced by the area of contact and this appears to override the influence of ploughing to give a lower coefficient of friction in the early stages of track formation. Of course this does not indicate that ploughing will be unimportant when sliding on a virgin ice surface.

##### 4.2. *The type of friction*

Our results are consistent with the view of Bowden & Hughes (1939) that water is formed at the area of contact and that it serves to lubricate the surfaces. If the water

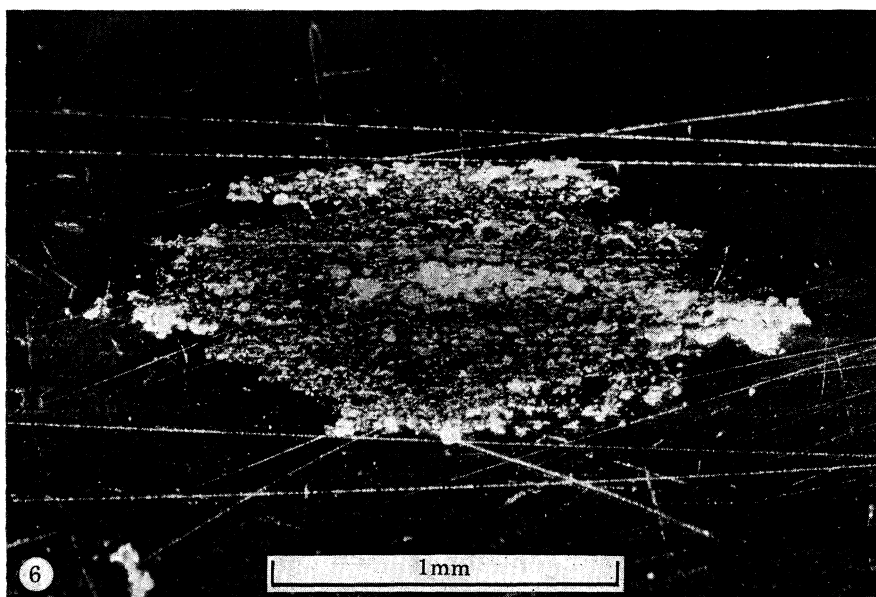
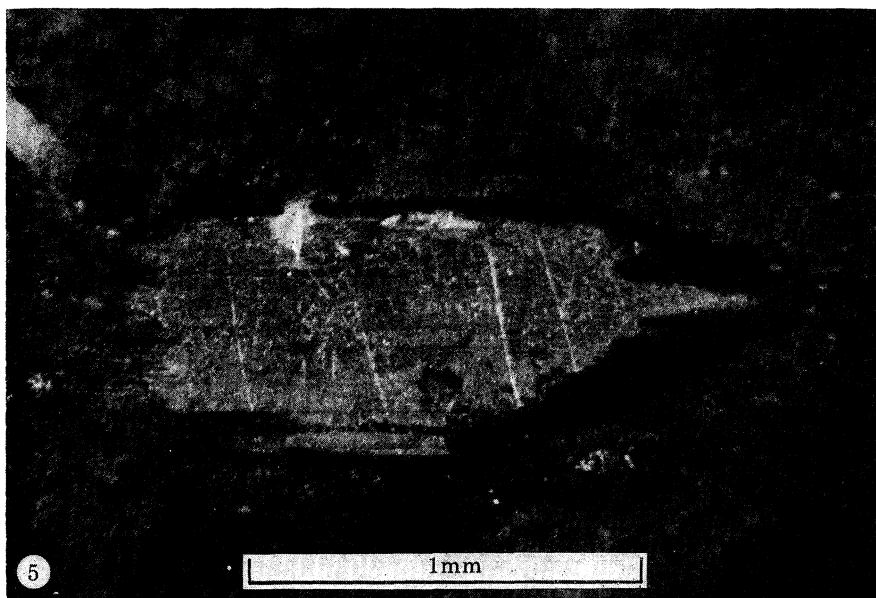


FIGURE 5. The area removed from a layer of soot on a brass rod sliding on the ice.  
The ice surface moved from left to right.

FIGURE 6. The area of contact of a Perspex rod after sliding on the ice.  
The ice surface moved from left to right.

separated the solid surfaces completely, the friction would arise solely from the viscous shearing of the water film. Using measured values of the coefficient of friction (0.025), normal load (11 N), area of contact ( $0.7 \text{ mm}^2$ ) and velocity ( $1 \text{ m s}^{-1}$ ), one can calculate the necessary value of the water-film thickness for this process. The result (5 nm) is much smaller than the surface roughness, and therefore viscous shearing of the water film cannot be the mechanism that produces the friction. (Putting the calculation another way round, if we assume a water film thickness of  $0.3 \text{ }\mu\text{m}$ , which we show later is the thickness melted by one passage of the slider, we find  $\mu = 0.0004$ , which is 60 times too small.) It is clear that mixed lubrication exists: the lubricant supports much of the load between the surfaces, but at high points the surfaces come into contact or are separated by a film only a few molecules thick, and these places are the source of most of the frictional force (Bowden & Tabor 1950, 1964). This view is supported by the observed wear of the rod surfaces; furthermore, the coefficients of friction measured in these and other experiments on ice lie in the range associated with mixed lubrication in other materials.

#### 4.3. *The frictional heating theory*

Because mixed lubrication exists the coefficient of friction can have a wide range of values depending on the ratio of fluid friction to solid contact. Since thin films of water exist at the contact, the ice surface will be at, or very close to, the melting temperature. Thus the frictional forces will automatically adjust themselves to ensure this condition. Therefore, to derive a coefficient of friction it is appropriate to analyse the problem in terms of heat balance rather than the physical mechanism of friction.

The additional plastic deformation or energy loss in elastic hysteresis that occurs in the experiments after the track has been formed is so small that sub-surface generation of heat is negligible, as we verify in §4.4. Thus we are concerned with frictional processes that generate heat essentially at the surface or (which is almost equivalent) in a very thin film of water. This means that, instead of considering the friction as a resistive force we may consider it as heat produced at the surface per unit displacement. To maintain the contact area at the melting point with the bulk of the ice and its surroundings at a lower temperature requires heat generation at the contact. We may calculate the heat required and hence the friction.

The total heat produced per unit displacement at each contact, in other words the frictional force,  $F$ , is the sum of three components:  $F_r$  the heat which is conducted through the rod,  $F_i$ , the heat which diffuses into the ice, and  $F_m$ , the heat used to melt the surface. Thus

$$F = F_r + F_i + F_m. \quad (4)$$

Since the water film will be above the melting point there will be an additional component arising from the specific heat of the water; it is convenient to regard this as part of  $F_m$ , and we shall show later that it is small, the temperature of the water being at most only a few kelvins above the melting point.

$F_r$ , the heat conducted through the rod

For the present we neglect the temperature difference just mentioned and regard the area of contact as fixed at the melting point. Then the rate of heat conduction through the rod per unit time will be proportional to the thermal conductivity  $k$  and to the difference between the ambient temperature  $T_0$  and the melting point  $T_m$  appropriate to the pressure. The heat conducted per unit time will be independent of the sliding velocity  $v$ . Therefore per unit displacement of the surfaces it will be inversely proportional to  $v$ . Thus

$$F_r = \frac{Ak(T_m - T_0)}{v}, \quad (5)$$

the constant  $A$  depending on the size of the contact area, the geometry of the rod and the nature of its surface.

$F_i$ , the heat diffusing into the ice

Assuming that the boundary condition that controls flow of heat into the ice is that the contact area must be at the melting point  $T_m$ , we can calculate the heat that diffuses into the ice. We first need to know how the depth of penetration of the temperature disturbance caused by the passage of the ice under the slider compares with the size of the contact area. If  $a$  is the length of the contact area, in time  $a/v$  the disturbance will have penetrated to a depth of order  $(Da/v)^{1/2}$ , where  $D$  is the thermal diffusivity of ice. With  $D = 1.2 \times 10^{-6} \text{ m}^2 \text{ s}^{-1}$ ,  $a = 1.5 \text{ mm}$  (as observed) and  $v = 3.0 \text{ m s}^{-1}$ , this depth is  $25 \mu\text{m}$ , which is only 1.6% of  $a$ . Because the depth of penetration is small compared with the size of the contact, the heat flow problem is essentially linear: that is, relative to the ice, the heat flows in straight lines normal to the surface, rather than spreading out radially. We therefore make the following assumption. As a small area of the ice, initially at temperature  $T_0$ , passes under the slider its temperature is suddenly raised from  $T_0$  to  $T_m$  and remains at  $T_m$  for a time  $a/v$ . We wish to know how much heat passes through the area during this time. Jaeger's exact calculation (1942) for the moving heat source allows for end effects but assumes the same heat flow from all points of the source rather than uniform temperature. Archard (1959) later used Jaeger's analysis to predict the temperatures attained by rubbing surfaces. For our purposes it is better to work from first principles. Since we may neglect end effects, the problem is essentially the following. A semi-infinite solid is initially at temperature  $T_0$  throughout; from time  $t = 0$  to  $t = a/v$  the temperature at the surface ( $z = 0$ ) is held at  $T_m$ . We have to calculate the heat that flows through unit area of the surface during this time.

The temperature  $T$  at time  $t$  and distance  $z$  from the surface is given by

$$T_m - T = (T_m - T_0) \operatorname{erf} z(4Dt)^{-1/2},$$

(see, for example, Carslaw & Jaeger 1959, p. 59). The rate of heat flow  $q$  per unit area into the body is

$$q = -k_1(\partial T/\partial z)_{z=0},$$

where  $k_i$  is the thermal conductivity of ice. Hence

$$q = k_i(T_m - T_0)(\pi Dt)^{-\frac{1}{2}}. \quad (6)$$

The total heat that flows through unit area from  $t = 0$  to  $t = a/v$  is therefore

$$Q = \int_0^{a/v} q dt = 2k_i(T_m - T_0)(a/\pi Dv)^{\frac{1}{2}}. \quad (7)$$

This gives the heat passing into unit area of the track during its passage under the slider. If the area of contact were rectangular with length  $a$ , and width  $b$  the heat passing per unit displacement, that is, per unit length of track, would be  $Qb$ , which by definition is  $F_i$ . Thus

$$F_i = Qb = 2k_i(T_m - T_0)b(a/\pi Dv)^{\frac{1}{2}}. \quad (8)$$

If the area of contact were elliptical,  $a$  and  $b$  now being the maximum length and breadth, equation (8) could be applied to each strip in the direction of sliding, the formula for  $F_i$  becoming:

$$F_i = 2k_i(T_m - T_0)(\pi Dv)^{-\frac{1}{2}} \int_{-\frac{1}{2}b}^{\frac{1}{2}b} x^{\frac{1}{2}} dy,$$

with  $x^2 = a^2(1 - 4y^2/b^2)$ . The integral is expressible in terms of gamma functions and we find

$$F_i = 1.74k_i(T_m - T_0)b(a/\pi Dv)^{\frac{1}{2}}. \quad (9)$$

Putting the expressions (5) and (9) for  $F_r$  and  $F_i$  in (4) we have the following equation for the frictional force

$$F = \frac{Ak(T_m - T_0)}{v} + \frac{B(T_m - T_0)}{v^{\frac{1}{2}}} + F_m, \quad (10)$$

where  $B = 1.74k_i b(a/\pi D)^{\frac{1}{2}}$ . The quantity measured most directly in the experiments is the coefficient of friction  $\mu$  rather than  $F$ . Accordingly we divide equation (4) by the normal load  $L$  and write  $\mu$  as the sum of three contributions

$$\mu = \mu_r + \mu_i + \mu_m, \quad (11)$$

where  $\mu_r = F_r/L$ ,  $\mu_i = F_i/L$ ,  $\mu_m = F_m/L$ . In the same way equation (10) becomes

$$\mu = \frac{Ak(T_m - T_0)}{Lv} + \frac{B(T_m - T_0)}{Lv^{\frac{1}{2}}} + \mu_m. \quad (12)$$

We cannot calculate explicitly the dependence of  $\mu_m$  on  $T_0$ ,  $v$  and  $k$ , but the following argument, which is crucial, allows us to deduce from the experiments an upper limit to its value, which turns out to be fairly small.

Since we are dealing with mixed lubrication the friction will be lower when there is more lubricating water present. If we assume that the greater the amount of water produced per unit displacement the more water will be present, it follows that lower values of  $\mu$  are associated with higher values of  $\mu_m$ . This principle enables us to deduce the behaviour shown in figures 7*a*, *b*, *c*. For example, in figure 7*a*,  $\mu_r$  and  $\mu_i$



both decrease with increasing  $T_0$ , as follows from equation (12). If we allowed  $\mu_m$  also to decrease we should violate the principle that lower  $\mu$  means higher  $\mu_m$ . Therefore  $\mu_m$  increases with  $T_0$ , as shown. The value of  $\mu$  at  $T_0 = T_m$ , which can be measured, thus represents an upper limit for  $\mu_m$  at temperatures below  $T_m$ .

In figures 7*b*, *c* a similar argument shows that  $\mu_m$  increases with  $v$  and decreases with  $k$ .

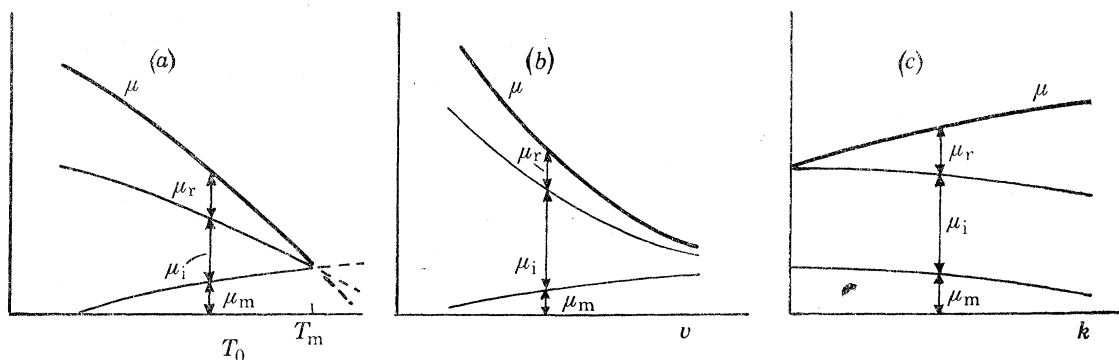


FIGURE 7. Showing diagrammatically how the coefficient of friction  $\mu$  varies with (a) the ambient temperature  $T_0$ , (b) the velocity of sliding  $v$ , (c) the thermal conductivity of the slider  $k$ .

#### 4.4. Comparison with experiment

By extrapolation to  $T_0 = T_m$  and  $v \rightarrow \infty$  we show below that the maximum value of  $\mu_m$  throughout our range of variables is 0.005. Thus  $\mu_m$  makes a fairly small contribution to  $\mu$  over much of the range.

The measured dependence of  $\mu$  on  $k$ , the thermal conductivity of the rod material, is seen in figure 3 or 4. The relative importance of the two terms in (12) corresponding to  $\mu_r$  and  $\mu_i$  depends on both  $k$  and  $v$ . It was found (§ 3.5) that for copper with  $v = 3.16 \text{ m s}^{-1}$  roughly half the total heat produced was conducted away through the rods; thus, for copper at this velocity, if we neglect  $\mu_m$ , we can say that  $\mu_r$  and  $\mu_i$  make roughly equal contributions to  $\mu$ .  $\mu_r$  is proportional to  $k$ , and  $k$  for copper is 2000 times  $k$  for Perspex.  $\mu_i$  does not depend on the rod material. Therefore  $\mu_r$  for Perspex is quite negligible at  $v = 3.16 \text{ m s}^{-1}$ , and it remains negligible down to the lowest velocity used ( $0.2 \text{ m s}^{-1}$ ). We conclude that, neglecting  $\mu_m$ ,  $\mu$  for Perspex equals  $\mu_i$  throughout the velocity range, and so the graphs of  $\mu$  for Perspex in figures 3 and 4 may be read as graphs of  $\mu_i$  for all materials.

The extent to which the values of  $\mu$  for mild steel and copper are greater than those for Perspex reflects the  $\mu_r$  term. In fact at  $v = 3.16 \text{ m s}^{-1}$ , as seen in figure 4, the values of  $\mu$  (copper)– $\mu$  (Perspex) are about 10 times greater than  $\mu$  (mild steel)– $\mu$  (Perspex) and this factor agrees with the ratio of the conductivities of copper and mild steel, 8.1, as it should do according to equation (12).

The fact that  $\mu_r \ll \mu_i$  for Perspex could have been foreseen without the experiment of § 3.5. The temperature far from the contact is  $T_0$  both in the ice and in the



slider rod, but in the ice fresh cold material is continually being brought close to the contact area. Thus the transient temperature gradients set up in the ice below the contact are necessarily much higher than the steady temperature gradients set up in the slider rod above the contact. This is the reason why most of the heat is lost by the route through the ice, unless the slider is much more highly conducting than ice.

Turning now to the dependence of  $\mu$  on the ambient temperature  $T_0$  (figure 4) we see that for mild steel and Perspex the linear dependence is as equation (12) would predict. For copper, where the  $\mu_r$  term contributes equally with  $\mu_i$ , we would

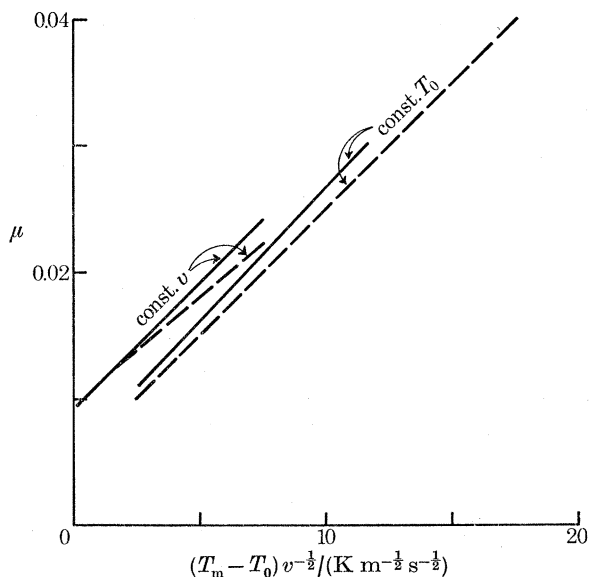


FIGURE 8. The variation of coefficient of friction with velocity and temperature for Perspex and mild steel. Total normal load ( $4L$ ) is 45.4 N. ----, Perspex rods; —, mild steel rods.

expect the slope of the line to be about twice that for Perspex, instead of about equal to it as drawn in figure 4. However, the scatter of the points is such that a line of considerably greater negative slope would still be consistent with the data. It would also be possible to adjust  $T_m$  in the expression for  $\mu_r$  to allow for the fact that the rod/water interface will be slightly above the melting point, but the slope of the line for copper is so uncertain that we cannot draw any conclusion about this from these observations.

For the dependence of  $\mu$  on  $v$  let us look first at the results in figure 3 for the mild steel and Perspex rods, where  $\mu_r$  can be neglected. The linear dependence of  $\mu$  on  $v^{-\frac{1}{2}}$  is predicted by equation (12). Equation (12) implies a relation between the linear dependence on  $v^{-\frac{1}{2}}$  and on  $T_0$ ; this has been tested by transcribing the lines in figure 3 and 4 for Perspex and mild steel on to a single graph of  $\mu$  against  $(T_m - T_0)v^{-\frac{1}{2}}$  in figure 8. The value of  $T_m$  was chosen to be  $-1.2^\circ\text{C}$  corresponding to the melting point of ice at the pressure measured in the experiment (see below). (The relative

positions of the lines are not very sensitive to the choice of  $T_m$  between  $-2$  and  $0^\circ\text{C}$ .) For each material the straight line for constant  $T_0$  ought to coincide with the straight line for constant  $v$ . In fact they have virtually identical slopes but slightly different intercepts. The intercepts differ by rather more than the experimental errors suggested by the scatter of the data points. This may be caused by a systematic error in the constant velocity runs resulting from the assumption that the equilibrium curve would lie midway between the heating and cooling curves. For this reason we prefer to obtain the maximum value of  $\mu_m$ , quoted earlier as 0.005, by extrapolating the constant  $T_0$  curves, rather than the constant  $v$  curves, to  $(T_m - T_0)v^{-\frac{1}{2}} = 0$ .

The dependence of  $\mu$  on  $v$  for copper will involve both the  $\mu_r$  term ( $v^{-1}$ ) and the  $\mu_i$  term ( $v^{-\frac{1}{2}}$ ). Thus we should not expect a straight line on a plot of  $\mu$  against  $v^{-\frac{1}{2}}$ . According to the results of §3.5 the terms are about the same at  $v = 3.16 \text{ m s}^{-1}$ ;  $\mu$  should tend to be proportional to  $v^{-1}$  at lower  $v$  and to  $v^{-\frac{1}{2}}$  at higher  $v$ . On a plot of  $\mu$  against  $v^{-\frac{1}{2}}$  the slope should increase with  $v^{-\frac{1}{2}}$ ; in figure 3 if the curve for copper is to make an intercept at about  $\mu = 0.005$  the slope would have to behave in this way.

The dependence of  $\mu$  on normal load  $L$  is not fully explicit in (12) because the load will alter the area of contact. This in turn will affect  $\mu_m$  in an unknown way, it will alter  $\mu_r$  by increasing  $A$  and it will alter  $\mu_i$  by increasing  $B$ . It will also alter  $T_m$ . The area of contact will increase approximately linearly with  $L$  if the ice surface deforms plastically. Assuming the shape of the contact area does not change, both dimensions  $a$  and  $b$  will increase proportionally to  $L^{\frac{1}{2}}$ , and  $\mu_i$  will then be proportional to  $L^{-\frac{1}{4}}$ . The  $L^{-\frac{1}{2}}$  behaviour observed is consistent with this conclusion within the experimental error.

Finally, we can make a numerical test of the last term  $\mu_i$  in equation (12) since all the quantities in it are measured. With  $k_i = 2.2 \text{ W m}^{-1} \text{ K}^{-1}$ ,  $b = 0.6 \text{ mm}$ ,  $a = 1.5 \text{ mm}$ ,  $D = 1.2 \times 10^{-6} \text{ m}^2 \text{ s}^{-1}$ ,  $T_0 = -11.5^\circ\text{C}$ ,  $L = 11 \text{ N}$ ,  $v = 1.0 \text{ m s}^{-1}$ , we find  $T_m = -1.2^\circ\text{C}$  and  $\mu_i = 0.048$ . Taking  $\mu_m = 0.005$  would give  $\mu = \mu_m + \mu_i = 0.053$ .  $\mu$  for Perspex, measured under these conditions, was 0.027, which is about half the calculated value.

The greatest uncertainty in calculating  $\mu_i$  is the area of contact. This is bound up with the problem of the thickness of the water film and we must now discuss these two questions. As the ice with its water film emerges from under the rod the water film will freeze in a distance comparable with the length of the contact area (the heat diffusion problem behind the contact area is something like the reverse of the one considered under the contact area). The thickness of this refrozen film is readily estimated since, in a steady state, it is equal to the thickness melted. The heat used in melting is  $\mu_m L$  per unit distance, and equating this with  $H\rho bc$ , where  $H$  is the latent heat,  $\rho$  is the density of ice,  $b$  is the width of the contact area and  $c$  is the thickness melted, we find (using  $\mu_m = 0.005$ ,  $L = 11 \text{ N}$ ,  $b = 0.6 \text{ mm}$ ) that  $c = 0.3 \mu\text{m}$ . This is a very small thickness. The water present at the area of contact may be thought of as made up of the small thickness of melt water just calculated, which builds up from front to rear, together with an unknown quantity which is simply

carried along with the slider. We have no clear way of estimating the amount of this entrained water except that the observation of wear of the rods suggests that it can be no more than a few micrometres. This is much less than the figure of  $70\ \mu\text{m}$  estimated by Bowden & Hughes (1939, p. 292), but they indicated that their measurements of electrical conductivity, although strong evidence for the presence of liquid, might not be an accurate indication of the thickness of the layer.

To obtain an idea of the depth of the track, and the additional distortion produced when the rod is in contact with the track, let us neglect the thickness of the water film and any shoulders formed at the sides of the track and consider a transverse

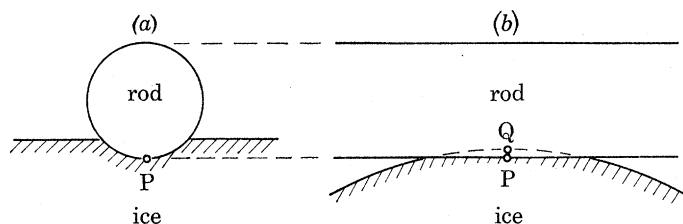


FIGURE 9. Sections through the rod-ice contact: (a) transverse, (b) longitudinal.

section at any one contact (figure 9*a*). From the radius of the rod and the observed width of the contact area one calculates that the edge of the track is  $9.0\ \mu\text{m}$  above the lowest point *P* of the rod. Figure 9*b* shows a longitudinal section perpendicular to the ice surface, which is assumed to be undisturbed except for the flat under the rod. From the radius of curvature of the ice surface (remembering that it is conical because of the V-groove) and the observed length of the contact area one calculates that the point *Q*, which would be on the bottom of the track if the rod were not there, is  $3.7\ \mu\text{m}$  above *P*. This is the amount of the temporary flattening produced by the rod. The depth of the track in the absence of the rod, is  $9.0 - 3.7 = 5.3\ \mu\text{m}$ . Thus the depth melted and then refrozen at each passage of the rod ( $0.3\ \mu\text{m}$ ) is only about 10% of the total flattening ( $3.7\ \mu\text{m}$ ). This accords with the view that most of the flattening produced by the passage of the rod is plastic or elastic distortion.

We can now verify that the plastic or non-recoverable elastic work expended in moving the flattened place on the ice is negligible compared with the work done in shearing at its surface. In a distance *a* the work of flattening by an amount *h* is certainly less, perhaps much less, than  $\frac{1}{2}Lh$ , compared with the work  $\mu La$  done by friction. The ratio is  $h/2\mu a \approx 0.05$ .

Even if there were only one rod one could not expect the refrozen surface to match precisely the transverse profile of the rod when it next passed under it. Still less will the surface match the rod profile when there are two rods. If the rods did not differ by more than about  $1\ \mu\text{m}$  the discrepancy might be taken up by elasticity of the two surfaces but greater differences, which will surely be present, will mean that the actual contact area will be less than the apparent area. To obtain agreement between the observed and calculated values of  $\mu_1$  entirely by adjusting the value of the width *b* (remembering that *b* also affects the pressure and therefore  $T_m$ )

requires  $b = 0.3$  mm instead of 0.6 mm as observed. Such a difference between real and apparent area seems quite reasonable.

We now consider the question of the temperature of the water film. The heat flux per unit time passing from the water into the ice surface is  $(\mu_m + \mu_i) Lv$ . If this were carried by conduction in the water it would require a temperature gradient of

$$\frac{(\mu_m + \mu_i) Lv}{Sk_w},$$

where  $S$  is the area of contact and  $k_w$  is the thermal conductivity of water. Putting in typical measured values gives a temperature gradient of  $1^\circ\text{C}/\mu\text{m}$ . Since the water film is not more than a few micrometres thick it follows that its average temperature is not more than a few degrees above the melting point.

In summary, we conclude that when the difference between the real and apparent contact area is taken into account (12) is consistent with the observations. The equation was deduced essentially from the postulate that the contact area is at the melting point. Thus the magnitude of the friction and its dependence on  $k$ ,  $T_0$  and  $v$  are all consistent with the notion that a film of water is present at the contact. The film of water is produced in our experiment by frictional heating, not by pressure melting. As Bowden & Hughes (1939) point out, if the film were produced by pressure melting, heat would have to flow to it not away from it: the temperature gradients are the wrong way round for this. In our experiments the lowering of the melting point by pressure merely means that the frictional heat at the contact has to heat the ice to a slightly lower temperature ( $-1.2^\circ\text{C}$ ) than would otherwise be the case.

On the other hand, at ambient temperatures very close to  $0^\circ\text{C}$  we should expect the temperature gradients to reverse in sign and pressure melting would then occur. The experiments by Barnes & Tabor (1966) show that the finite hardness of ice limits the possible pressure, and under the conditions of our experiments would limit pressure melting to temperatures between  $-2$  and  $0^\circ\text{C}$ . If then the surroundings of the contact were warmer than the contact itself, but still below  $0^\circ\text{C}$ , pressure melting could take place. In this case equation (12) still holds,  $T_m - T_0$  being negative and therefore  $F_r$  and  $F_i$  being negative. Rearranging (4) to read

$$F - F_r - F_i = F_m,$$

we see that the heat of friction adds to the heat received at the contact through the rod and the ice to produce the heat used in melting (see the broken lines in figure 7*a*). The terms  $-(F_r + F_i)$  can be regarded as the contribution of pressure melting to the total heat  $F_m$  used in melting the lubricating film.

It is possible to go a little further with our model and ask how  $\mu$  is distributed within the area of contact. Equation (6) shows that the rate of flow of heat  $q$  into unit area of the ice under the slider is proportional to  $t^{-\frac{1}{2}}$ , where  $t$  is the time measured from the instant that the area meets the slider. The friction contribution  $\mu_i$  at each point is related to  $q$  by  $\mu_i v p = q$ , where  $p$  is the local pressure. So  $\mu_i$  is propor-

tional to  $t^{-\frac{1}{2}}$  and thus to  $s^{-\frac{1}{2}}$ , where  $s$  is the distance from the leading edge of the contact area. Thus, if edge effects are ignored,  $\mu_i$  and the heat flow  $q$  are both theoretically infinite at the leading edge of the contact. The measured friction is, of course, the average of  $\mu$  over the contact area and this is finite. The real situation may well be that there is an area of dry friction at the leading edge where the temperature of the ice is being rapidly raised from  $T_0$  to the melting point, thereby avoiding the infinity and *reducing* the total friction below the previously calculated value. We can estimate the size of this effect by using linear heat conduction theory and calculating the time needed to raise the surface temperature from  $T_0$  to  $T_m$ . With a steady flow of heat per unit area,  $q$ , the time  $t$  is given by

$$T_m - T_0 = \frac{2q}{k_i} \left( \frac{Dt}{\pi} \right)^{\frac{1}{2}}$$

(Carslaw & Jaeger 1959, p. 75). If  $\mu_d$  is the coefficient of dry friction,  $q = \mu_d v p$ , where  $p$  is the pressure, assumed uniform. It follows that the heating by dry friction takes place over a length  $s_d$  given by

$$s_d = \frac{\pi k_i^2 (T_m - T_0)^2}{4 \mu_d^2 p^2 D v}. \quad (13)$$

The value to take for  $\mu_d$  is rather uncertain. If we adopt 0.2 as a conservative estimate and take other numerical values as before we find  $s_d = 35 \mu\text{m}$ , which is 2% of the observed length  $a$  of the contact area. From this it would follow that the contribution to the total friction of such a dry region at the leading edge is about 8% ( $\mu_d = 0.1$  would give 17%, while  $\mu_d = 0.5$  would give 3%).

Thus while a dry region may explain part of the discrepancy noted above, where  $\mu$  (calculated) was 0.053 and  $\mu$  (observed) was 0.027, it seems that the major part must still be attributed to the difference between the real and apparent contact areas.

We conclude that, in the range of our experiments, the main contribution to the observed friction comes from a large lubricated area at the melting point rather than from a small dry area in front, but of course at low enough temperatures or small enough velocities the dry area would certainly become the significant one. By putting  $s_d = a$  in equation (13), one can estimate very roughly that completely dry friction would occur at about  $T_0 = -70^\circ\text{C}$  at  $v = 1 \text{ m s}^{-1}$  or at  $v = 20 \text{ mm s}^{-1}$  when  $T_0 = -10^\circ\text{C}$ , but these estimates, of course, are subject to the uncertainty in the value of  $\mu_d$ , taken here as 0.2.

Precisely how the heat is generated in the lubricated area, and what is the detailed mechanism that produces the frictional drag are questions that are not answered by our experiments. Indeed the experiments show that the same friction would be produced by any mechanism which allowed the contact area to be at the melting point and which led to the main heat loss being by conduction ( $\mu_r$  and  $\mu_i$ ) rather than by melting ( $\mu_m$ ). Putting the matter another way, if we *know* that the



contact is at the melting point and  $\mu_m$  is small, we can calculate the friction, but to understand *why* these conditions hold would need a deeper insight into the frictional mechanism.

#### 4.5. *Real ice skating*

Real ice skating takes advantage not only of the low friction parallel to the skate, which is necessary for speed, but the high friction perpendicular to the skate, which is necessary for control. Obviously one should not try to deduce optimum conditions for skating without taking both into account. So far as the low friction parallel to the skate is concerned there are two main differences between the experiments with rods and real skating. First the geometry of the contact areas is different, and second the rods do not slide on a virgin ice surface. The first difference was investigated by using the curved ice skate and comparing its behaviour with that of the rods. Considering the difference in the two geometries, the results showed remarkable similarity (figure 3) both in the coefficient of friction and in its dependence on velocity. This suggests that the mechanisms of friction may be the same in the two cases, but without knowing more about the nature of the contact area between the curved skate and the ice one cannot be sure.

The fact that ice skating occurs on a virgin ice surface is important from the point of view of the contribution of a ploughing term to the frictional force. In our experiments no significant ploughing term is present because measurements were made after the tracks had been formed. In the early stages of track formation we observed lower coefficients of friction, indicating that the additional ploughing term was more than balanced by a reduction in the other contribution. This is probably explained by the reduced area of contact when sliding takes place on a virgin surface. The hardness of ice at a given temperature depends on the time of application of the indenter (Barnes & Tabor 1966). Whereas in our experiments a given place on the ice was subjected to repeated loadings amounting to a total loading time of up to 10 s, a single passage of the slider would have given a loading time of less than 1 ms. A shorter loading time means a smaller area of contact. This has two effects: provided the ambient temperature  $T_0$  is below the melting point  $T_m$  at the contact, it decreases the heat losses by decreasing the constants  $A$  and  $B$  in equation (12), and, by increasing the pressure it lowers the melting point  $T_m$ . Both effects reduce the coefficient of friction; the lowering of the melting point means that in the early stages of track formation pressure-melting would have occurred at lower temperatures. On the other hand, if  $T_0$  were greater than  $T_m$  (pressure-melting), a smaller area of contact hinders heat flow to the contact and so *increases* the coefficient of friction.

Thus in ice skating one can identify the following effects on the friction. Ploughing tends to increase friction by requiring more plastic deformation. However, ploughing may also increase the area of contact. The short loading time associated with sliding on a virgin surface has the opposite effect of decreasing the area of contact. If the net effect is to decrease the area,  $\mu$  will decrease (by decreased heat losses) if  $T_0 < T_m$ , but will increase (by reduced heat gains in pressure-melting) if  $T_0 > T_m$ .



## 5. SUMMARY AND CONCLUDING REMARKS

A direct calculation of the shearing force between rubbing surfaces is very hard, particularly in systems where mixed lubrication takes place, the difficulty being to devise a suitable model of the surfaces. When we consider the friction of ice the physical picture is further complicated by the fact that ice makes its own lubricant. However, one important piece of information is automatically known in this case: the coexistence of ice and water at the contact area implies that it is at the melting point. This information enabled us to approach the calculation of frictional force from a completely different direction. Instead of estimating the energy expended in shearing the interface, we calculated the energy leaving the contact area in the form of heat.

Neglecting the small amount of energy expended in plastic deformation below the surface, the heat generated at the contact area per unit relative displacement must be equal to the frictional force. The heat is dissipated in three ways: the latent heat of the melt-water produced in sliding, conduction into the slider rod, and diffusion into the ice. We argued (§4.3) that as the latent heat term increases the friction must decrease, because of the additional water. This enabled us to show that in our experiments the latent heat term was comparatively small. The high *transient* temperature gradients in the moving ice remove heat more efficiently than the lower *steady* temperature gradients in the stationary slider rod, unless the slider rod has a much higher thermal conductivity than that of ice. Accordingly, when Perspex and steel rods were used in the experiments diffusion into the ice was considerably larger than conduction into the rods, and this component of the heat dissipation therefore controlled the value of the coefficient of friction. Because the temperature at the contact is fixed at the melting point, the way in which this component (and therefore the friction) varied with velocity and temperature could be simply calculated. Putting values for the dimensions of the contact area and the thermal constants of ice into the calculated expression gave a value for the coefficient of friction agreeing, within a factor of two, with the experimental value. The discrepancy between experiment and theory is probably due to overestimation of the area of contact.

The magnitudes of the other two components of the heat dissipation under various conditions were obtained empirically. The final expression (12) for the coefficient of friction, containing all three components, accounts for all the significant features of the experimental results including the behaviour of the copper rods, which is different from that of the other materials because of their high thermal conductivity.

Does this analysis also apply to other materials? Ice is not exceptional in exhibiting very low kinetic friction near its melting point. Experiments by Bowden & Hutchison (1939) on the friction of solids sliding on benzophenone (m.p. 49°C) and dinitrobenzene (m.p. 89°C) and by Bowden & Rowe (1955) on solid krypton, gave results similar to those on ice. Benzophenone expands on melting (International Critical Tables 1928) and there is no evidence that dinitrobenzene does not do

likewise. Bowden & Rowe suggested that some pressure melting might occur with krypton because it contracted on melting. However, according to Landolt-Börnstein (1971), the sign of the density change on melting is not anomalous for krypton, the densities being  $3.0 \text{ Mg m}^{-3}$  for the solid and  $2.6 \text{ Mg m}^{-3}$  for the liquid, and so pressure melting is not a possibility. Low kinetic friction near the melting point in fact seems to be a general property of materials, as would be expected on the frictional melting theory. We should remember, however, that if the hardness of the material drops appreciably near the melting point the area of contact will increase; this will increase the heat losses and the friction will be correspondingly greater. In addition, a drop of hardness will increase the ploughing term when sliding takes place on a virgin surface.

The experimental work described was done as an undergraduate project, the design of the apparatus being based on experience gained in earlier (unpublished) projects carried out by P. W. Davies, B. K. Lynas, R. J. Morgan and I. Newell. We thank Professor D. Tabor, F.R.S., for his helpful suggestions during the preparation of the manuscript.

#### REFERENCES

- Archard, J. F. 1959 The temperature of rubbing surfaces. *Wear* **2**, 438–455.
- Barnes, P. & Tabor D. 1966 Plastic flow and pressure melting in the deformation of ice I. *Nature, Lond.* **210**, 878–883.
- Bowden, F. P. & Hughes, T. P. 1939 The mechanism of sliding on ice and snow. *Proc. R. Soc. Lond. A* **172**, 280–298.
- Bowden, F. P. & Hutchison, R. F. 1939 (unpublished) Quoted by F. P. Bowden and D. Tabor in *The friction and lubrication of solids*, Part I (1950), p. 70, and part II (1964), p. 152. Oxford: Clarendon Press.
- Bowden, F. P. & Rowe, G. W. 1955 The friction and mechanical properties of solid krypton. *Proc. R. Soc. Lond. A* **228**, 1–9.
- Bowden, F. P. & Tabor, D. 1950 *The friction and lubrication of solids*, Part I. Oxford: Clarendon Press.
- Bowden, F. P. & Tabor, D. 1964 *The friction and lubrication of solids*, Part II. Oxford: Clarendon Press.
- Carslaw, H. S. & Jaeger, J. C. 1959 *Conduction of heat in solids*, 2nd ed. Oxford: Clarendon Press.
- International Critical Tables 1928 *International Critical Tables of Numerical Data, Physics, Chemistry and Technology*, vol. 4, p. 16. New York: McGraw Hill.
- Jaeger, J. C. 1942 Moving sources of heat and the temperature at sliding contacts. *Proc. R. Soc. N.S.W.* **56**, 203–224.
- Landolt-Börnstein 1971 Numerical data and functional relationships in science and technology, new series, group III, vol. 6, p. 13.
- Mellor, M. 1974 A review of basic snow mechanics. International Association of Hydrological Sciences, Commission of Snow and Ice, Symposium on Snow Mechanics, Grindelwald 1974.
- Reynolds, O. 1901 Papers on mechanical and physical subjects II, p. 737. Cambridge University Press.



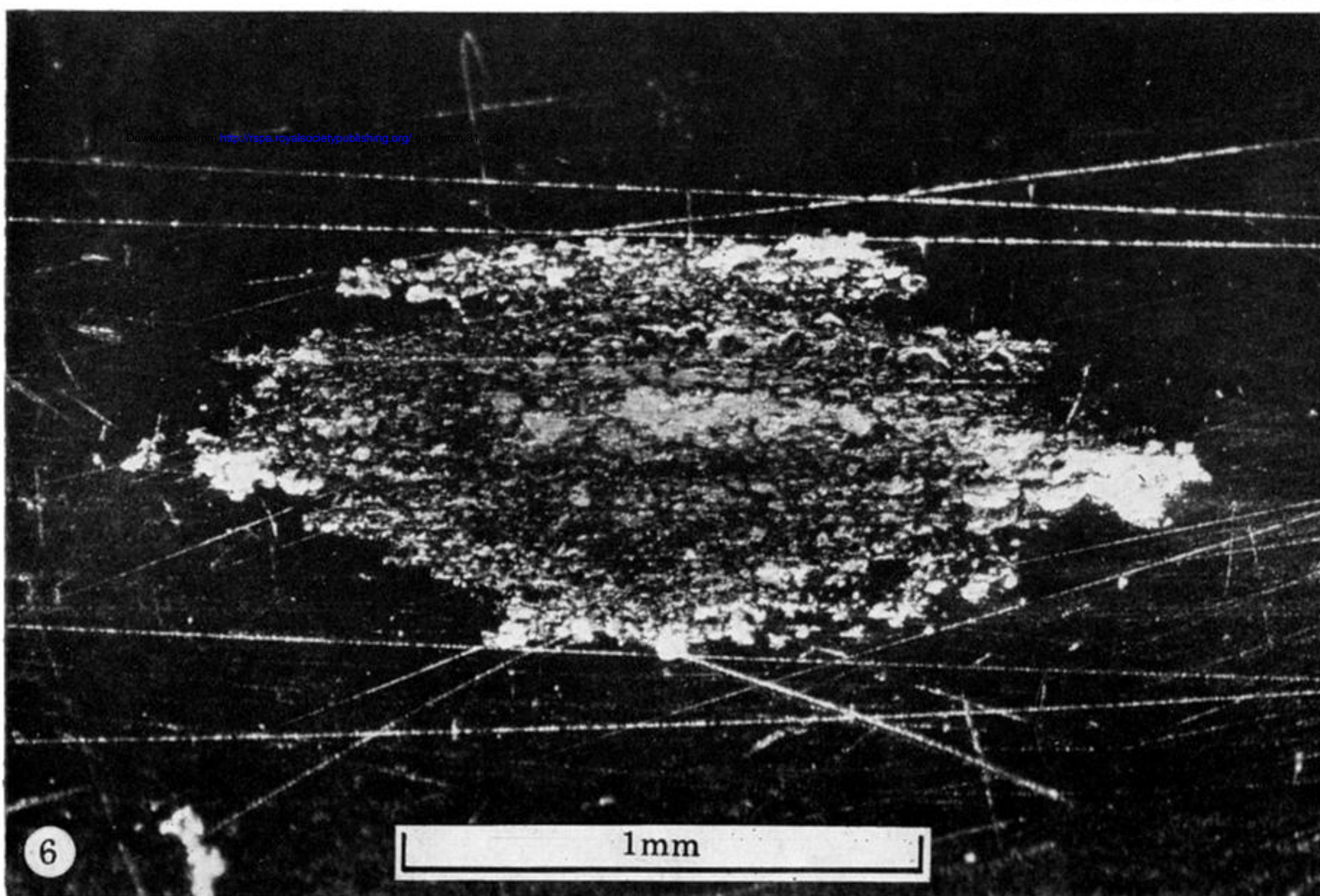
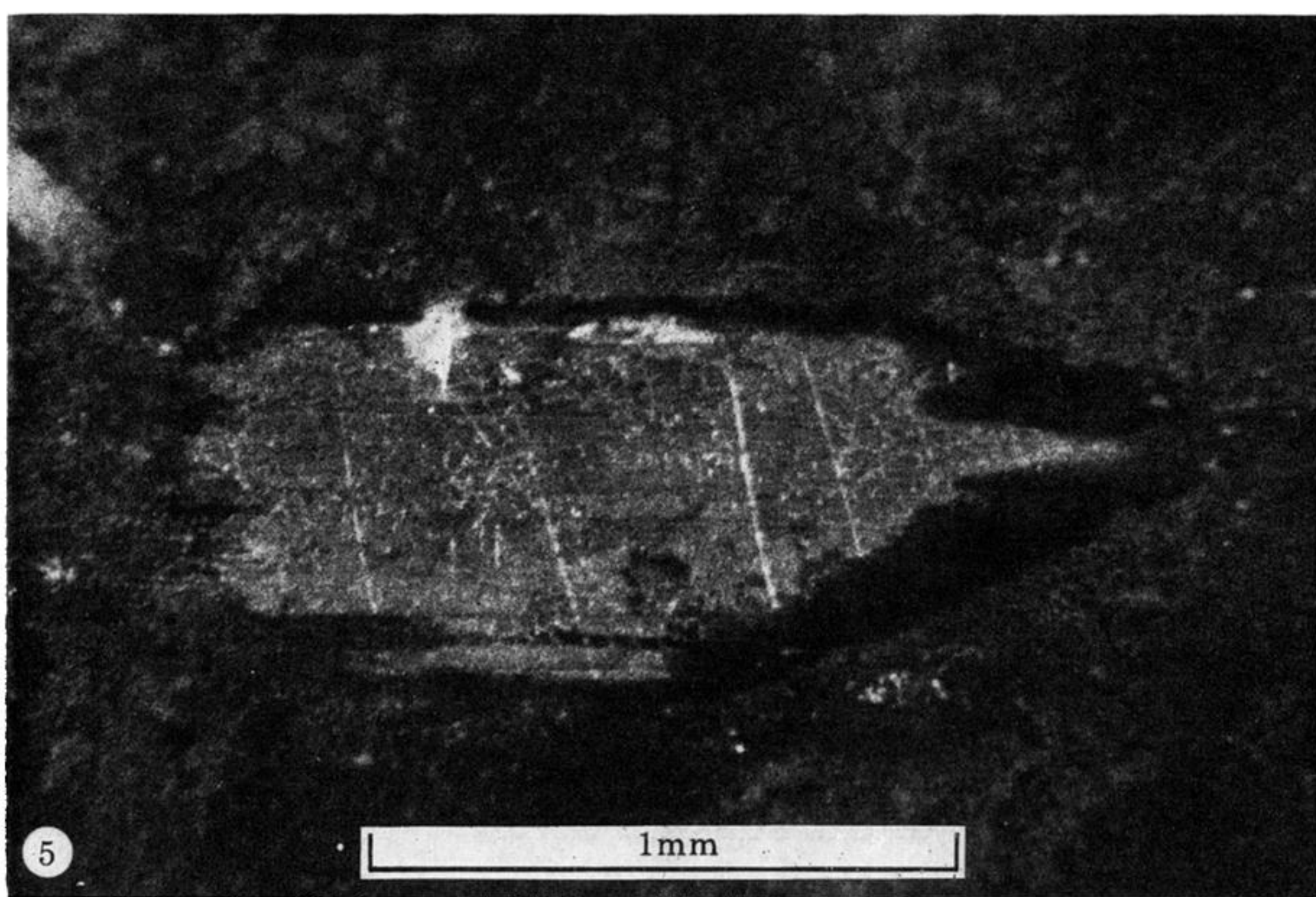


FIGURE 5. The area removed from a layer of soot on a brass rod sliding on the ice.  
The ice surface moved from left to right.

FIGURE 6. The area of contact of a Perspex rod after sliding on the ice.  
The ice surface moved from left to right.